J. Cent. South Univ. (2015) 22: 2691−2698
DOI: 10.1007/s11771-015-2799-9

Springer

Reinforcement strength reduction in FEM for mechanically stabilized earth structures

XUE Jian-feng(薛剑峰)[1, 2], CHEN Jian-feng(陈建峰)[1]

1. Key Laboratory of Geotechnical and Underground Engineering of Ministry of Education (Tongji University), Shanghai 200092, China;
2. School of Applied Science and Engineering, Monash University, Victoria 3842, Australia

Abstract: The factor of safety of mechanically stabilized earth (MSE) structures can be analyzed either using limit equilibrium method (LEM) or strength reduction method (SRM) in finite element/difference method. In LEM, the strengths of the reinforcement members and soils are reduced with the same factor. While using the SRM, only soil strength is reduced during the calculation of the factor of safety. This causes inconsistence in calculating the factor of safety of the MSE structures. To overcome this, an iteration method is proposed to consider the strength reduction of the reinforcements in SRM. The method is demonstrated by using PLAXIS, a finite element software. The results show that the factor of safety converges after a few iterations. The reduction of strength has different effects on the factor of safety depending on the properties of the reinforcements and the soil, and failure modes.

Key words: mechanically stabilized earth structures; factor of safety; strength reduction method; iterative method

1 Introduction

Mechanically stabilized earth (MSE) structures are often used in the construction of railway tracks, road embankment, bridge abutment and retaining structures. It is favoured by many geotechnical projects due to its low cost, construction time efficiency, high tolerance to differential settlement and versatile aesthetical finishes etc [1−4]. The design and analysis methodologies have been included in various guidelines and standards [5−7]. In the design of the MSE structures, the stability of the structure is one of the main factors that need to be checked.

SIMAC et al [8] describes that the failure of the MSE structures can take place solely within the reinforced zone, outside the reinforced zone or within the facing, which are named as internal, external (global) or facing failure. Later, MORRISON et al [9] detailed the failure mechanism and included compound failure, in which the slip surface passes through the reinforced zone and the unreinforced soils. In the analysis of stability of MSE structures, the internal, global and the compound failures are the main concerning of geotechnical engineers. And the facing failure can be normally avoided by quality control during construction. For external, internal or compound stability, the analysis can be performed using either limit equilibrium method (LEM) or strength reduction method (SRM) incorporated in finite element (FE) or finite differential (FD) methods, which are available in many commercial softwares, e.g., Geostudio, ReSSA, PLAXIS and FLAC.

The stability of the MSE structures is described with factor of safety, f, which is defined as

$$f = \frac{r(c,\ \phi, T)}{d} \tag{1}$$

where d is disturbance; r is resistance; c, ϕ and T are the cohesion, friction angle and tensile strength of the reinforcements, respectively. In LEM analysis, the factor of safety is calculated using the method of slice developed for slope stability analysis by including the resistance from the reinforcement inclusions. Take the geogrid reinforced slope in Fig. 1 as an example, using simplified Bishop method of slice [10], the factor of safety of the slope can be defined as

$$f = \frac{\sum_{i=1}^{n}(N_i \tan\phi + c\Delta l_i)R + \sum_{j=1}^{m} T_j y_j}{\sum_{i=1}^{n}(w_i \sin\theta_i)R} \tag{2}$$

where f is the factor of safety of the slope; $N_i = w_i\cos\theta_i$; w_i is the weight of the ith slice; θ_i is the inclination angle

Foundation item: Project(41072200) supported by the National Natural Science Foundation of China; Project(14PJD032) supported by the Shanghai Pujiang Program, China
Received date: 2014−06−24; **Accepted date:** 2014−09−10
Corresponding author: CHEN Jian-feng, Professor, PhD; Tel/Fax: +86−21−65983545; E-mail: jf_chen@tongji.edu.cn

of the base of the ith slice; Δl_i is the arc length of the ith slice; R is the radius of the failure circle; c is the cohesion of the soil at the base of the ith slice; ϕ is the friction angle of the soil at the base of the ith slice; T_j is the allowable tensile strength of the jth reinforcement; y_j is the moment arm for the jth reinforcement; n is the number of slices; m is the number of reinforcement layers.

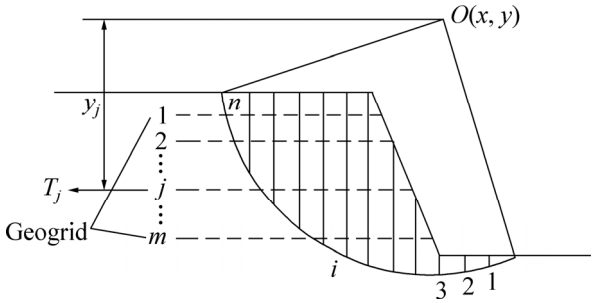

Fig. 1 Method of slice in a geogrid reinforced soil slope

LEM analysis is widely accepted by engineers and practitioners due to its simplicity. But in LEM, the critical slip surface is normally predefined to follow a certain surface. And different assumption on the inter-slice reaction may result in different factor of safety [11]. In complex situation, e.g., MSE walls on soft ground, the dissipation of excess pore water pressure, stress redistribution due to the inclusion of reinforcement members, and the strength increment due to consolidation can not be considered in LEM [12−14]. However, SRM incorporated in FE or FD method overcomes the disadvantages in LEM, and can provide further information about deformation of the structure and simulate the construction process of the structure. Therefore, SRM is widely used in the design of many types of soil structures, such as retaining walls and braced excavations [15−18].

In SRM, the factor of safety of a structure is examined by reducing the soil strength parameters with a factor till the structure reaches the limit state [19]. In the SRM, the stability of the structure is evaluated by

$$f = \frac{c}{c_r} = \frac{\tan\phi}{\tan\phi_r} \tag{3}$$

where c and ϕ are the cohesion and friction angle of the soil, respectively; c_r and ϕ_r are the reduced cohesion and friction angle, respectively.

Comparing Eqs. (2) and (3), we can see that only soil strength parameters are reduced in the SRM. While in LEM, the strengths of both the soil and the reinforcements are reduced by the factor of safety at limit state. Such inconsistence in the definitions may lead to misinterpretation of the stability of the structures in some cases. As strength reduction method is a general method used to analyze the stability of soil structures, in many cases, the reduction of the strength of structural members has less effect on the stability of the system especially when the strength of the material is very high (e.g. steel or concrete) or is analyzed separately, e.g. retaining walls. Therefore, the reduction of reinforcement strength was not included in the SRM. But for geogrid reinforced soil slopes or walls, the result from SRM may overestimate the factor of safety of the structure. This work proposes an iterative method to consider the reduction of strength of the reinforcements while using FEM. The method is demonstrated with a number of geogrid reinforced soil slopes. It was found that the reduction of geogrid strength and stiffness has different results in the factor of safety of the MSE slopes, depending on the soil and geogrid properties.

2 Reinforce mechanism of MSE slopes

Soil is a particulate material and its strength is strongly affected by the confining pressure. For cohesionless soils, a slope steeper than the soil's natural impose angle is impossible without considering suction effect. By laying layers of reinforcements, e.g., geogrids, among soils, slopes can be built with steeper angles to a higher height, and can support higher loads, e.g., higher traffic loads or even bridges. In a reinforced soil slope, the reinforcements provide confinement to prevent soil deformation and thus provide confining pressure to soils. This results in stress redistribution within the structure. The potential displacement in soils causes tensile, shear or bending of the reinforcements. Relative moment between soil particles and the reinforcement results in a shear resistance along the soil and reinforcement interface and subsequently tensile stress in the reinforcements. If the shear resistance is not large enough, pulling out failure of reinforcement may occur. A weaker reinforcement may result in a tensile failure of the reinforcement [20]. In the design of MSE structures, tensile failure is normally considered to avoid overdesign [6].

The stiffness of the reinforcements is another factor that controls the performance of the MSE structures. By analyzing a number of soils slopes, CHENG et al [14] found that the stability of soil slopes is less sensitive to the elastic modulus of soils as the stiffness of soils does not contribute much to resistance in Eq. (1). While in MSE structures, research showed that the stiffness of the geogrid may increase the overall stiffness of the reinforced soil zone, and thus the factor of safety of the structure, particularly of the structure on soft soils [21].

BATHURST et al [22] proposed a working stress method to analyze the safety of the MSE walls using the working strain to obtain the working stress within the reinforcement using the related reinforcement stiffness value. They used global and local stiffness to consider the variation of the reinforcement stiffness in the design as the stress distribution within soils and the reinforcement at working conditions differs from those at limit state.

3 Proposed method

As described in Eq. (3), the factor of safety of a soil structure is calculated by $c-\phi$ reduction in FE or FD method. During this process, the strength of non-soil material remains unchanged. Therefore, the SRM is anticipated to result in a higher factor of safety, without considering the reduction of the strength of the geogrid as considered in the LEM in Eq. (2).

To account for the reduction of geogrid strength in the SRM, the factor of safety of the MSE structures is defined as

$$f=\frac{c}{c_{\mathrm{r}}}=\frac{\tan\phi}{\tan\phi_{\mathrm{r}}}=\frac{T}{T_{\mathrm{r}}} \tag{4}$$

where T is the tensile strength of the geogrid, and T_{r} is the reduced strength of the reinforcement.

As in the current SRM, the reduction of reinforcement strength can not be considered, an iterative method is proposed. In the proposed method, the factor of safety of the MSE structures is calculated using the standard method firstly. Then, the strength of the geogrids is reduced by a factor of the calculated factor of safety. Using the reduced strength, a new factor of safety value will be obtained by carrying out a second $c-\phi$ reduction calculation. Then, the procedure continues until the factor of safety value converges. The procedure is shown in the flow chart in Fig. 2.

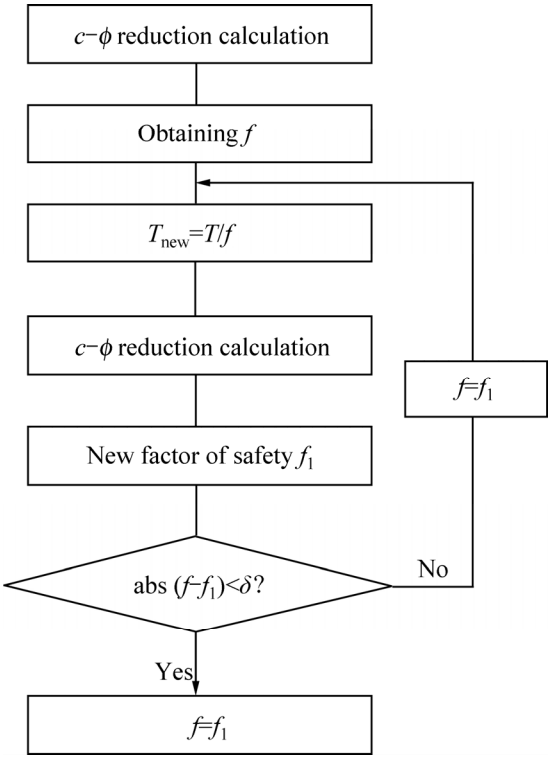

Fig. 2 Flow chart of iterative process

4 Application of proposed method

One example is introduced in the following sections to demonstrate the method of strength reduction of reinforcement materials during the FE analysis. The FE analysis was carried out on a PLAXIS 2D platform (version 2011). The factor of safety of the slope was analyzed using the SRM incorporated within PLAXIS. As the main purpose of the paper is to discuss the strength reduction of reinforcement, the results are therefore not further compared with results from LEM.

4.1 Performing strength reduction in FEM

The main slope is 5 m high with a slope of 2H:5V, with a 1 m high shoulder at a slope of 2:1 (H:V) as shown in Fig. 3. The properties of the retained soil and the foundation soil are also shown in Fig. 3 with the slope geometry as used in the FEM model. Elastic-perfectly plastic Mohr−Coulomb criterion was used to model the retained and foundation soil. Two cases with different types of geogrid materials were considered in the example: a higher strength material with the axial stiffness J=620 kN/m and the tensile strength T=35 kN/m in case 1 and a relatively lower strength geogrid with J=400 kN/m and T=11.8 kN/m in case 2. The length of the geogrid is 7 m with 2 m of wrapped around segment on the wall facing. The geogrid reinforcements are installed at an interval of 0.5 m in vertical. The reinforcements were modeled as elastoplastic material, using geogrid element in PLAXIS. The soil-geogrid

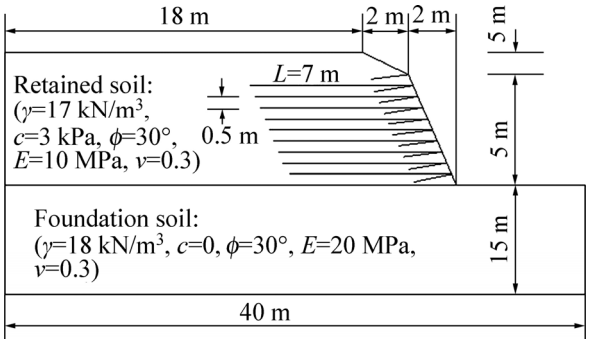

Fig. 3 A geogrid reinforced slope and model size used in PLAXIS

interface was modeled with bilinear Mohr−Coulomb model, and the interface properties are taken from soil using a resistant ratio. The resistance ratio was taken as 0.8 in the analysis.

The factor of safety of the slopes was analyzed using the procedure introduced in Fig. 2. The parameters used in each step and results of each step are shown in Table 1. During the reduction of geogrid properties in each iteration the soil input parameters remains unchanged. It is shown that a few iteration steps may be required for factor of safety to converge during the reduction of the geogrid strength and stiffness. And the reduction of factor of safety due to the reduction of the geogrid properties varies from case to case. In the case of the stronger geogrid, the factor of safety of the slope only reduces 4.2%, while for the case of relatively weaker geogrid, a reduction of 11.5% in the factor of safety of the slope is observed by considering the reduction of geogrid strength and stiffness. This suggested that the factor of safety can be well misinterpreted without considering the reduction of geogrid strength.

Table 1 Procedures to calculated factor of safety using iteration process

Case	Iteration step	Geogrid strength/(kN·m^{-1})	f	Δf
1	Step 1	35	1.797	4.2%
	Step 2	19.5	1.714	
	Step 3	20.4	1.722	
2	Step 1	11.8	1.582	11.5%
	Step 2	7.5	1.336	
	Step 3	8.8	1.423	
	Step 4	8.3	1.391	
	Step 5	8.4	1.497	
	Step 6	8.45	1.401	

Δf is the difference in factor of safety.

4.2 Stress redistribution in reinforcement members

The maximum axial stresses in the geogrid members before and after the reduction of the geogrid properties were analyzed and the results of case 1 are listed in Table 2. It can be seen from the results that axial stresses increased in all the geogrid members. After the reduction of the geogrid properties, more members reached the ultimate strength at the limit state. This means that the reduction of the strength of the geogrids changed the stress redistribution in the soils and the geogrids. While in case 2, which is not shown in the table, the stress levels in the geogrid members all reached the ultimate strength both before and after reduction. In this case the strength of the material is lower; therefore, the reduction of strength has significant effect on the factor of safety of the slope as shown above.

Table 2 Stress distribution in geogrids before and after reduction of geogrid strength in case 1

Geogrid No. (from top)	Maximum tensile stress/(kN·m^{-1})	
	Before reduction	After reduction
1	29.28 (83.66%)	20.23 (99.66%)
2	16.18 (46.22%)	17.06 (84.04%)
3	19.59 (55.97%)	12.86 (63.35%)
4	19.74 (56.4%)	19.92 (98.13%)
5	20.27 (57.91%)	16.66 (82.06%)
6	25.11 (71.74%)	20.3 (100%)
7	28.8 (82.29%)	20.3 (100%)
8−10	35 (100%)	20.3 (100%)

4.3 Change of failure mechanism of slopes

The critical slip surfaces of the two slopes before and after the reduction of the strength of the geogrid are shown in Figs. 4 and 5. The figures show that the reduction of geogrid strength may change the failure mechanism of the slopes depending on the material properties.

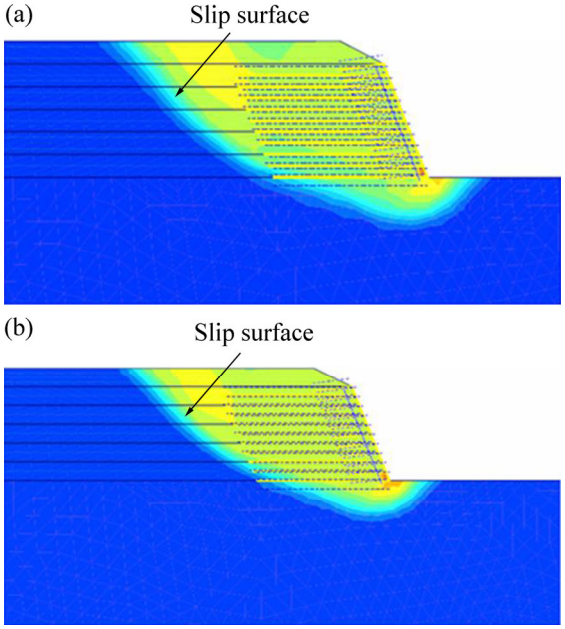

Fig. 4 Critical slip surfaces of case 1: (a) Before reduction of geogrid strength; (b) After reduction of geogrid strength

In Fig. 4, the failure mechanism remains almost unchanged after the reduction. This may be due to the fact the geogrid is strong and stiff, so as it is hard for slip surface to form within the reinforced soil body. This may also suggest that when the global failure is in form, the strength of geogrid has little effect on the factor of safety of the slope, which has been shown in the previous discussions. This will most likely result in an over design.

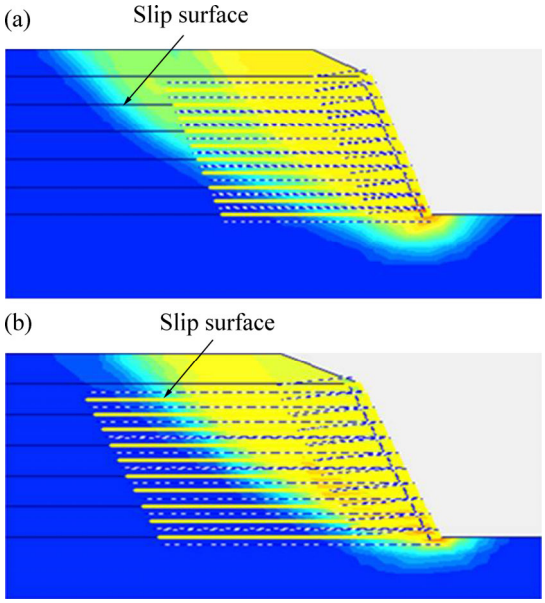

Fig. 5 Critical slip surfaces of case 2: (a) Before reduction of geogrid strength; (b) After reduction of geogrid strength

While in Fig. 5(a), before reduction of geogrid strength, the critical slip surface takes a form of compound failure. After reduction of geogrid strength, the slide follows the mode of internal failure as shown in Fig. 5(b). This also explains why the strength of the geogrid has much influence on the factor of safety of the structure as listed in Table 1.

The example shows that the reduction of the geogrid strength has different effects on the failure mechanism of the reinforced slopes. This will be discussed further in the next case study.

5 Case study

A 7.6 m high geogrid reinforced soil wall, with wrapped-around vertical facing, was considered in this case. The wall was constructed as a temporary retaining structure in Shanghai Botanic Garden, Shanghai, China [23]. The wall was constructed at the end of a road section. The road embankment is 37.2 wide on top, with a 1.5*H*:1*V* side slope. The profile of the embankment is shown in Fig. 6(a).

The site consists of 5 compressible soil layers within the depth of 31 m from the ground level, which are (from top to bottom): silty clay layer (2.6 m thick), mucky silty clay layer (4.4 m thick), clay layer (3.6 m thick), silty clay layer (7.4 m thick) and silty clay layer (13.0 m thick). The ground water table is only within 0.5 m below the ground surface. The geotechnical properties of the soils are summarized in Table 3.

Before the construction of the wall, a 1.6 m thick preliminary fill was laid onto the ground to compensate for the expected settlement during construction. Then, a 0.6 m thick sand cushion was laid onto the preliminary fill for drainage using medium sand compacted to a bulk density of 17.0 kN/m^3. Prefabricated vertical drains (PVDs) were installed in a triangle pattern at a center to

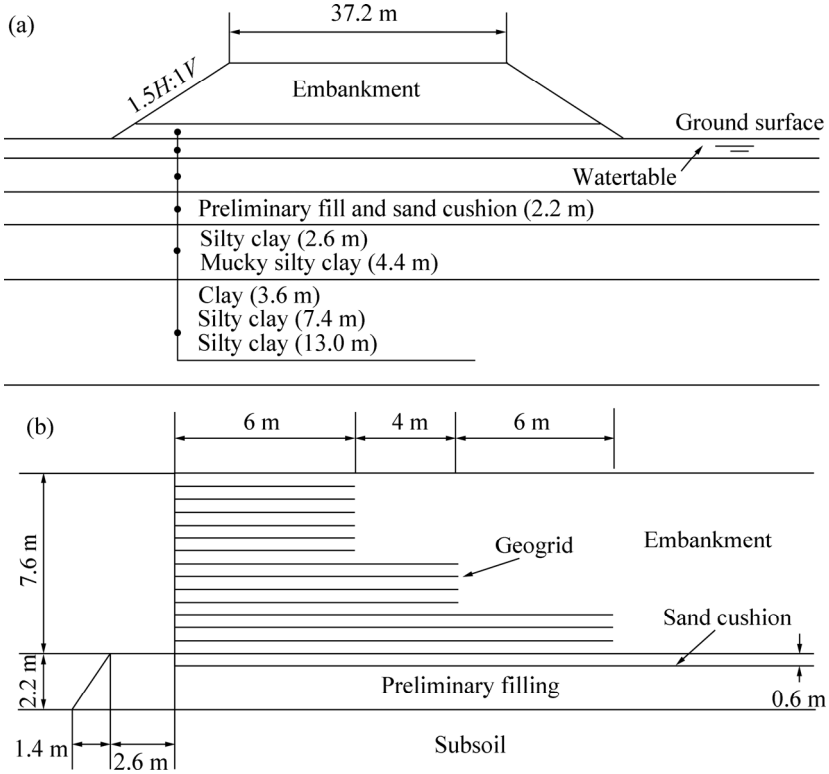

Fig. 6 Geometry of road and reinforced wall at Shanghai Botanic Garden: (a) Cross section of road embankment; (b) Geometry and geogrid layout of reinforced wall

Table 3 Summary of geotechnical properties of subsoil

Layer	γ/(kN·m^{-3})	w_n/%	I_p/%	e_0	c'/kPa	ϕ'/(°)	E_{50}^{ref} / MPa	k_h/(10^{-9} m·s^{-1})	k_v/(10^{-9} m·s^{-1})
1	18.4	32.5	16.2	0.93	7.0	27.9	3.18	16.0	1.14
2	17.9	38.0	15.1	1.06	7.0	28.0	2.12	16.4	1.08
3	17.5	41.1	18.0	1.16	6.0	24.9	2.47	13.9	1.33
4	19.5	24.0	15.1	0.70	17	29.8	8.37	1.6	0.12
5	19.3	25.2	15.1	0.73	18	31.2	5.70	1.6	0.12

Note: γ is the unit weight; w_n is the natural water content; I_p is the plasticity index; e_0 is the initial void ratio; c' is the effective cohesion; ϕ' is the effective friction angle; E_{50}^{ref} is the secant modulus in standard drained triaxial test; k_h is the horizontal permeability; k_v is the vertical permeability.

center spacing of 1.5 m to a depth of 12 m below the ground surface. The silty clay from the top layer was used as the preliminary fill and the backfill for the wall. The fill was compacted to the bulk density of 19.0 kN/m^3 using bulldozer and road roller. Once the settlement caused by the preliminary fill and sand cushion was stabilized, the construction of the wall started.

The wall was reinforced with 15 layers of high density polyethylene (HDPE) uniaxial geogrid at an interval of 0.5 m in depth. The axial stiffness of the geogrid was 620 kN/m at 5% strain, and the rupture strength was 70 kN/m. The original design of the reinforcement was 10 m long with 3.5 m of wrapped around segment. But the wall failed after the placement of the last layer of the soil. Back analysis showed that at the construction speed, the factor of safety of the wall is only 1.04 without considering the weight of the machinery [24]. As the failure mechanism of the wall is not the main purpose of this work, a new reinforce system is designed to show the method developed above. The layout of the reinforcement is shown in Fig. 6(b). The construction procedure is shown in Fig. 7.

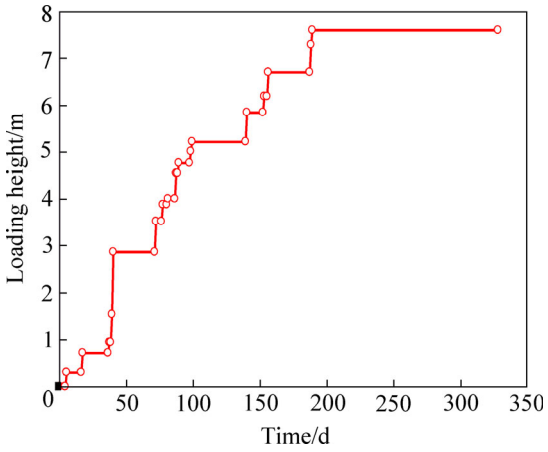

Fig. 7 Fill height with time

The preliminary fill, the sand cushion, and the RSW backfill were modeled with linear elastic-perfectly plastic Mohr−Coulomb model. And the underneath soft foundation soils are modeled with the hardening-soil model to consider the increment of soil strength due to consolidation. The three-dimensional axisymmetrical water flow problem in the PVD drained soils was transformed into a plane strain problem using the technique proposed by HIRD et al [25]:

$$k_{hp} = \frac{2}{3} \cdot \frac{B^2}{{D_e}^2} \cdot \frac{1}{\mu} \cdot k_h \tag{5}$$

where k_h is the horizontal permeability of subsoil; k_{hp} is the equivalent horizontal permeability of the drainage system in plane strain condition; B is the width of the plane-strain unit cell, which is 1.5 m in this case; D_e is the diameter of the effective zone of drainage, and 1.58 m is used in the analysis, which is 1.05 times the spacing of the drains; μ is a dimensionless factor related to smear effect, and can be calculated by

$$\mu = \ln(D_e / d_s) + k_h / k_s \ln(d_s / d_w) - 0.75 \tag{6}$$

where d_s and d_w are the diameters of the smeared zone and the drain, respectively; k_s is the horizontal permeability in the smeared zone. As recommended by CHAI and MIURA [26], the diameter of the smeared zone d_s was taken as 3 times the mandrel's equivalent diameter, which is 110 mm. The equivalent diameter d_w of the band shaped PVD was adopted as the average of its width and thickness, which are 100 mm and 4 mm, respectively. The ratio of k_h and k_s was 13.5 as recommend by SHEN et al [27]. Substituting the values above into Eq. (5), a value of k_{hp}=0.023k_h was obtained for the numerical modelling.

The factor of safety of the wall was 1.170 without considering the reduction of geogrid strength. After three iteration steps considering the reduction of the strength of the geogrid, the factor of safety of the wall converged to 1.155. It seems that the properties of the geogrid have little effect on the factor of safety of the wall in this case, but the failure mechanism of the wall changed from global failure to compound failure after the reduction of the strength as shown in Fig. 8. Thus, the change of the factor of safety does not only depend on the failure modes as shown in the previous example but also the overall contribution of geogrids and the soils to the resistance against sliding.

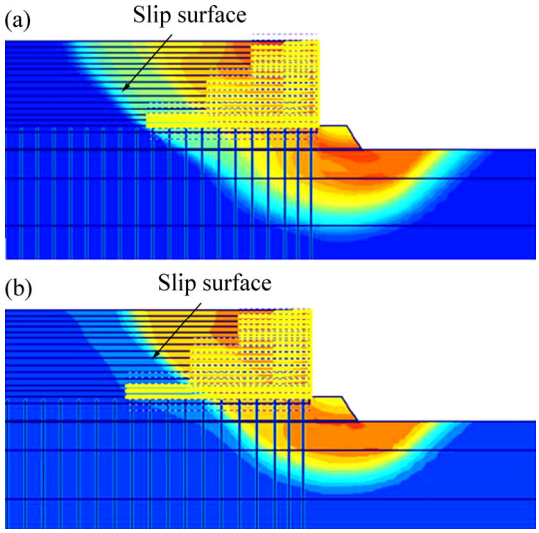

Fig. 8 Deformation of wall after $c-\phi$ reduction: (a) Before reduction of geogrid strength; (b) After reduction of geogrid strength

6 Conclusions and recommendation

In the design of mechanically reinforced soil structures using strength reduction method in FEM, the reduction of strength of the reinforcements is not considered in LEM method. This may result in an overestimation of factor of safety of the reinforced soil structure as shown in the example and the case study. The proposed iterative method allows the consideration of strength reduction of the reinforcements in FEM analysis.

It is found that the reduction of the strength of the reinforcement inclusions has different effects on the factor of safety of structures. For conditions when only global shear failure occurs, the strength reduction of the reinforcements may have little influence on slope stability since the reinforcements do not participate in the sliding. In cases when compound failures or internal failure occurs, the reduction of reinforcement strength may have different effects on the factor of safety of a structure depending on the overall contribution of reinforcements and the soils to the resistance against sliding, even if the failure mode is global before the reduction of reinforcement strength. However, the reduction of reinforcement strength in SRM can generally result in a lower factor of safety. It is recommended that further studies should be carried out on the choice of the reduction of strength of the reinforcements in FEM analysis.

References

[1] LEE Z Z, WU J T H. A synthesis of case histories on GRS bridge-supporting structures with flexible facing [J]. Geotextiles and Geomembranes, 2004, 22(4): 181−204.

[2] YOO C, JUNG H S. Measured behaviour of a geosynthetic-reinforced segmental retaining wall in a tiered configuration [J]. Geotextiles and Geomembranes, 2004, 22(5): 359−376.

[3] LIU C N, YANG K H, HO Y H, CHANG C M. Lessons learned from three failures on a high steep geogrid-reinforced slope [J]. Geotextiles and Geomembranes, 2012, 34(6): 131−143.

[4] CHEN J F, YU S B. Centrifugal and numerical modeling of a reinforced limestabilized soil embankment on soft clay with wick drains [J]. ASCE, Int J Geomech, 2011, 11(3): 167−173.

[5] American Association of State Highway and Transportation Officials (AASHTO). Standard specifications for highway bridges [S]. 17th ed. 2002.

[6] BS8006. Code of practice for strengthened/reinforced soils and other fills [S]. 2010.

[7] Federal Highway Administration (FHWA) FHWA-NHI-10-024. Design and construction of mechanically stabilized earth walls and reinforced soil slopes [S]. 2009.

[8] SIMAC M R, BATHURST R J, BERG R R, LOTHSPEICH S E. Design manual for segmental retaining walls (Modular Concrete Block Retaining Wall Systems [S]. 1st ed. Herndon, VA, USA: National Concrete Masonry Association (NCMA), 1993: 250.

[9] MORRISON K F, HARRISON F E, COLLIN J G, DODDS A, ARNDT B. Shored mechanically stabilized earth (SMSE) wall systems design guidelines [R]. Report No. FHWA-CFL/TD-06-001, Washington D.C: Federal Highway Administration, 2006.

[10] BISHOP A W. The use of the slip circle in the stability analysis of slopes [J]. Geotechnique, 1955, 5: 7−17.

[11] FREDLUND D G, KRAHN J, PURAHL D E. The relationship between limit equilibrium slope stability methods [C]// Proceedings of the 10th International Conference on Soil Mechanics and Foundation Engineering. Rotterdam: A. A. Balkema, 1981: 409−416.

[12] DAWSON E M, ROTH W H, DRESCHER A. Slope stability analysis by strength reduction [J]. Geotechnique, 1999, 49(6): 835−840.

[13] CALA M, FLISIAK J. Slope stability analysis with FLAC and limit equilibrium methods [C]// FLAC and Numerical Modelling in Geomechanics. Rotterdam: A.A Balkema, 2001: 111−114.

[14] CHENG Y M, LANSIVAARA T, WEI W B. Two-dimensional slope stability analysis by limit equilibrium and strength reduction methods [J]. Computers and Geotechnics, 2007, 34(3): 137−150.

[15] MATSUI T, SAN K C. Finite element slope stability analysis by shear strength reduction technique [J]. Soils and Foundations, 1992, 32: 59−70.

[16] GRIFFITHS D V, LANE P A. Slope stability analysis by finite elements [J]. Geotechnique, 1999, 49: 387−403.

[17] DAWSON E, MOTAMED F, NESARAJAH S, ROTH W. Geotechnical stability analysis by strength reduction [C]// Slope Stability 2000. Reston, Virginia: American Society of Civil Engineers, 2000: 99−113.

[18] CHEN J F, LIU J X, XUE J F, SHI Z M. Stability analyses of a reinforced soil wall on soft soils using strength reduction method [J]. Engineering Geology, 2014, 177: 83−92.

[19] BRINKGREVE R B J, ENGIN E, SWOLFS W M. PLAXIS 2D manual [M]. Delft: Plaxis B V, 2012.

[20] TEIXEIRA S H C, BUENO B S, ZORNBERG J G. Pullout resistance of individual longitudinal and transverse geogrid ribs [J]. Journal of Geotechnical and Geoenvironmental Engineering, 2007, 133(1): 37−50.

[21] SKINNER G D, ROWE R K. Design and behaviour of a geosynthetic reinforced retaining wall and bridge abutment on a yielding foundation [J]. Geotextiles and Geomembranes, 2005, 23(4): 234−260.

[22] BATHURST R J, ALLEN T M, WALTERS D L. Reinforcement loads in geosynthetic walls and the case for a new working stress design method [J]. Geotextiles and Geomembranes, 2005, 23: 287−322.

[23] XUE J F, CHEN J F, LIU J X, SHI Z M. Instability of a geogrid reinforced soil wall on thick soft Shanghai clay with prefabricated vertical drains: a case study [J]. Geotextiles and Geomembranes, 2014, 42(4): 302−311.

[24] CHEN J F, LIU J X, XUE J F, SHI Z M. Failure analyses of a reinforced embankment by strength reduction and limit equilibrium methods considering hardening of soft clay [J]. KSCE J Civ Eng, 2014, 18(7): 2043−2050.

[25] HIRD C C, PYRAH I C, RUSSELL D, CINICIOGLU F. Modeling the effect of vertical drains in two-dimensional finite element analyses of embankments on soft ground [J]. Can Geotech J, 1995, 32(5): 795−807.

[26] CHAI J C, MIURA N. Investigation of factors affecting vertical drain behavior [J]. J Geotech Geoenviron, 1999, 125(3): 216−226.

[27] SHEN S L, CHAI J C, HONG Z S, CAI F X. Analysis of field performance of embankments on soft clay deposit with and without PVD-improvement [J]. Geotextiles and Geomembranes, 2005, 23(6): 463−485.

(Edited by YANG Hua)